Probing Galaxies through Quasar Absorption Lines
Proceedings IAU Colloquium No. 199, 2005
P. R. Williams, C. Shu, and B. Ménard, eds.

doi:10.1017/S1743921305002565

The distribution and baryon content of H I absorbers at $z < 0.5$

N. Lehner[1], B. D. Savage[1], B. P. Wakker[1], K. R. Sembach[2], and T. M. Tripp[3]

[1]Department of Astronomy, University of Wisconsin, 475 North Charter Street, Madison, WI 53706, USA
email: nl@astro.wisc.edu, savage@astro.wisc.edu, wakker@astro.wisc.edu

[2]Space Telescope Science Institute, 3700 San Martin Drive, Baltimore, MD 21218, USA
email: sembach@stsci.edu

[3]Department of Astronomy, University of Massachusetts, Amherst, MA 01003, USA
email: tripp@fcrao1.astro.umass.edu

Abstract. We combine FUV spectra obtained with *FUSE* and STIS/E140M of HE 0226–4116 ($z = 0.495$), PG 1116+215 ($z_{\rm em} = 0.177$), and PG 1259+593 ($z_{\rm em} = 0.478$) to determine the distribution of column density and Doppler width of the Lyα absorber population at $z < 0.5$ detected in the spectra of these 3 quasars. The high spectral resolution UV spectra allow us to derive simultaneously the redshift, column density, and Doppler width of each absorber. Two different populations of H I absorbers appear to be present: narrow and broad H I absorptions that could be tracers of the warm photoionised IGM ($T < 10^5$ K) and warm-hot ionised medium (WHIM, $T \sim 10^5 - 10^6$ K). For a reliable assessment of the baryonic content of the Lyα forest at low z it is crucial to determine the relative numbers of photoionised absorbers vs. hot collisionally ionised absorbers. Preliminary results indicate that 30–40% of the total baryons are in the photoionised IGM and at least 20% in the WHIM. We also discuss the observed evolution of the Doppler parameter with redshift.

1. Introduction

Observations of Lyα absorption lines in the spectra of QSOs provide a highly sensitive probe of the evolution and the distribution of gas in the Universe from high to low redshift. Many H I absorption lines at different redshifts occur along a QSO sight-line with $\log N({\rm H\,I}) < 17$, known as the Lyα forest. To follow the evolution with redshift of the Lyα forest is critical for an understanding of the evolution and formation of the structures in the Universe. At $z \gtrsim 1.5$, observations of the Lyα forest are obtained from ground-based telescope, typically with 8–10 m class telescopes (Hu *et al.* 1995; Lu *et al.* 1996; Kim *et al.* 1997, 2002a), but at $z \leqslant 1.5$ it requires UV space-based instruments. Space-based UV astronomy has produced remarkable results (firstly by the discovery itself of the Lyα forest at low redshift, Bahcall *et al.* 1991), but most of the UV studies have lacked the spectral resolution and wavelength coverage of the higher redshift studies (Weymann *et al.* 1998; Impey *et al.* 1999; Penton *et al.* 2000, 2004), requiring, in particular, assumptions for the Doppler parameter to derive the column density.

With recent observations of several QSOs with the Space Telescope Imaging Spectrograph (STIS) in the echelle E140M mode at good signal-to-noise (S/N) per resolution element ($\sim$7 km s^{-1}, comparable to the spectral resolution of the high redshift studies), we can now derive accurately the fundamental parameters of the Lyα forest lines (redshift z, column density N, and Doppler parameter b) and directly compare these

parameters and their distributions with those of high redshift samples that have similar spectral resolution. Not only has the quality of the data improved compared to previous UV studies, but moreover, the full FUV-UV wavelength coverage provided by STIS and *FUSE* along each line of sight produces several Lyman series and metal lines, making the line identification reliable and giving an unprecedented insight into the physical conditions and metallicity. The typical STIS/E140M S/N per resolution element is 10, 15, and 24 for HE 0226–4110, PG 1116+215, and PG 1259+593 respectively. The S/N is not constant over the full wavelength ∼1216 Å to ∼1730 Å available with STIS/E140M; in particular it deteriorates rapidly at $\lambda > 1600$ Å. The detection limit depends on the S/N and the breadth over which the spectrum is integrated. We estimate that our sample is complete for $\log N(\mathrm{H\ I}) \gtrsim 13.20$ or in the rest frame equivalent width $W_{1215} \simeq 88$ mÅ. A complete description of these sight-lines can be found in Lehner *et al.* (2005, in preparation), Richter *et al.* (2004), and Sembach *et al.* (2004).

2. Distribution and evolution of *b*

The Doppler parameter b has been used to constrain the temperature of the Lyα forest. At high redshift, it is believed that absorbers are predominantly broadened by the Hubble flow, although thermal broadening is not negligible. At low redshift, since the reionisation epoch is far enough in the past, the IGM should have returned to an equilibrium ionisation equilibrium. However, although a substantial fraction of baryons may remain in the cooler photoionised gas, a large fraction of the baryons are believed to be present in the shock-heated gas at $T \sim 10^5 - 10^6$ K as predicted by models (Cen & Ostriker 1999; Davé *et al.* 1999). Observationally, the low redshift WHIM has been detected and studied mostly via O VI absorption (Tripp *et al.* 2004), but also via Ne VIII in the spectrum of HE 0226–4110 (Savage *et al.* 2005), and X-ray absorption in the spectrum of Mkn 421 (Nicastro *et al.* 2005).

Another way of detecting the 10^5 to 10^6 K WHIM has recently emerged from studies of IGM absorption observed with the E140M mode of STIS: the broad Lyα absorbers first discovered toward PG 1259+593 and PG 1116+215 (Richter *et al.* 2004, Sembach *et al.* 2004). While most of these broad Lyα absorbers are metal-less and could trace the WHIM in the cosmic web, some have been discovered with associated O VI that could trace gas associated with galaxies. The first example of a broad H I/narrow O VI pair was found at $z = 0.31978$ in the PG 1259+593 sight-line (Richter *et al.* 2004). The nearly factor of 4 difference in b-values of O VI and H I strongly suggests that the H I and O VI lines are purely thermally broadened, with $T{=}3.6^{+1.7}_{-1.4}{\times}10^5$ K. Several good examples of broad H I absorptions are also observed in multiple Lyman series lines. Earlier studies with lower spectral resolution and smaller wavelength coverage have failed to discover the broad Lyα absorption (Penton *et al.* 2004).

Comparison with previous low redshift studies:

The median b in our sample is larger than the medians found in the low redshift IGM by Davé & Tripp (2001) and Shull *et al.* (2000). Davé & Tripp (2001) used automated software to derive b and N, not allowing the search for broader components. Shull *et al.* (2000) only went after the Lyβ absorption lines in the *FUSE* wavelength to combine with known Lyα absorption lines observed with GHRS. Davé & Tripp (2001) found a median and mean b-value of 22 $\mathrm{km\,s^{-1}}$ and 25 $\mathrm{km\,s^{-1}}$ respectively. If we restrict our sample to data with $b \leqslant 40$ $\mathrm{km\,s^{-1}}$, the median, mean and dispersion are 28 $\mathrm{km\,s^{-1}}$ and 27 ± 7 $\mathrm{km\,s^{-1}}$, which compare well with those derived by Shull *et al.* (2000).

https://doi.org/10.1017/S1743921305002565 Published online by Cambridge University Press

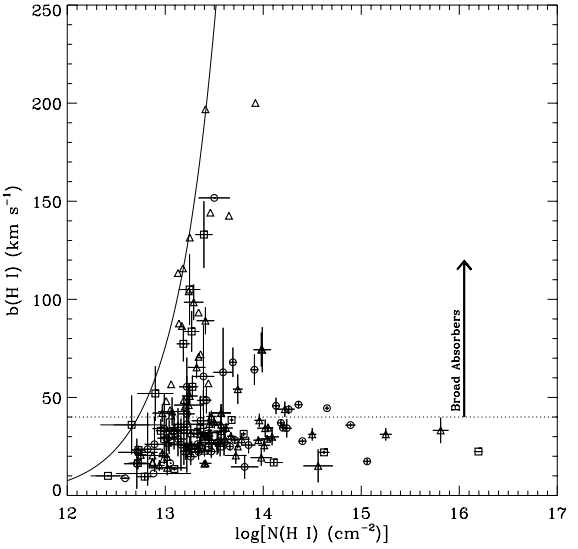

Figure 1. Line width versus H I column density for the Lyα absorbers along the HE 0226–4110 (*circles*), PG 1116+215 (*squares*), and PG 1259+593 (*triangles*) sight-lines. Data with no error bars are uncertain. The solid line shows b vs. N(H I) for a Gaussian line with 10% central optical depth – absorption lines to the left of this line are not detectable.

Comparison with high redshift systems:

A prediction made by hydrodynamical simulations of structure formation is that the percentage of gas in the 10^5–10^6 K WHIM increases as the Universe evolves. Hence, we should observe a larger fraction of H I absorbers with large b at low redshift than at high redshift if the broadening is dominated by thermal motions. In Fig. 1 we show the $b - \log N$(H I) plot for the 3 considered sight-lines. This figure suggests the existence of two branches. The high b branch may be tracing H I in the lower temperature portion of the WHIM, whereas the low b branch may correspond to the photoionised IGM. This will need to be confirmed by adding many more QSO sight-lines to have better statistics. At high redshift the plot of $b - \log N$(H I) looks like a scatter plot with the presence of a lower envelope (e.g. Kim *et al.* 2002b).

In Fig. 2, we compare the number distribution of b(H I) for $z < 0.5$ and redshifts $1.5 \leqslant z \leqslant 3.6$ obtained from observations with similar spectral resolution (Hu *et al.* 1995; Kim *et al.* 2002a). The low redshift sample shows a tail of high b(H I) absorbers that is not seen at high redshift, consistent with the hydrodynamical simulations of structure formation. For $b > 40$ km s^{-1} the fraction of broad Lyα absorbers is 0.33 (48/145) at $z < 0.5$, while it is 0.18 (601/3408) at $1.5 \leqslant z \leqslant 3.6$. For $b > 60$ km s^{-1} the fraction of broad Lyα absorbers at $z < 0.5$ is 3.2 times larger than at $1.5 \leqslant z \leqslant 3.6$. The median value of the distribution shown in Fig. 2 is also higher for the low redshift sample (32 km s^{-1}) than for the high redshift sample (26 km s^{-1}). Although our sample is currently small, it strongly suggests an increasing of b with decreasing redshift and a larger fraction of systems with $b > 40$ km s^{-1} at low-z than at high-z. We note, however, that because the high redshift IGM is so crowded with narrow Lyα absorption lines, broad Lyα lines are intrinsically more difficult to find and their physical parameters more uncertain than at low redshift.

https://doi.org/10.1017/S1743921305002565 Published online by Cambridge University Press

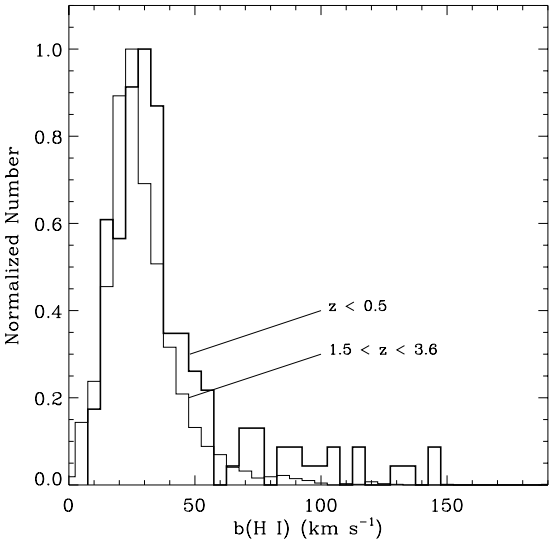

Figure 2. Comparison of the normalised distribution of b(H I) for the low z sample (dark solid histogram) and for the high redshift ($1.5 \leqslant z \leqslant 3.6$) samples from Hu *et al.* (1995) and Kim *et al.* (2002). Each sample has a similar spectral resolution (7–8 km s^{-1}), but the low redshift sample has 145 absorbers compared to 3,408 absorbers in the high redshift sample.

3. The baryon density of the low redshift Lyα forest

3.1. *Narrow Lyα absorption lines*

To estimate the baryon content of the photoionised Lyα forest we follow the method presented by Schaye (2001). The mean gas density relative to the critical density can be obtained from the H I density distribution function through the relation, assuming the gas is isothermal:

$$\Omega(\mathrm{NLy}\alpha) \approx 2.2 \times 10^{-9} h^{-1} \Gamma_{12}^{1/3} T_4^{0.59} \int_{N_{\min}}^{N_{\max}} N_{\mathrm{H\,I}}^{1/3} f(N_{\mathrm{H\,I}}) dN_{\mathrm{H\,I}}, \tag{3.1}$$

where $h \equiv H_0/(100\,\mathrm{km\,s^{-1}\,Mpc^{-1}})$ is the Hubble constant, Γ_{12} is the H I photoionisation rate in units of 10^{-12} s^{-1}, T_4 is the IGM temperature in units of 10^4 K, and $f(N_{\mathrm{H\,I}})$ the differential column density distribution. We use $\Gamma_{12} \approx 0.05$ (Davé & Tripp 2001), $T_4 \approx 2.3$ (where we follow Davé & Tripp who estimated that $b_{\mathrm{thermal}} \approx 0.7b$, with $b = 28$ km s^{-1} the median and mean value of our sample with $b \leqslant 40$ km s^{-1}), and $h = 0.7$ (Spergel *et al.* 2003). A maximum-likelihood fit to our data implies $f(N_{\mathrm{H\,I}}) \equiv C_{\mathrm{H\,I}} N_{\mathrm{H\,I}}^{-\beta} \approx 6.3 \times 10^{10} N_{\mathrm{H\,I}}^{-1.7}$. We first assume that only H I absorbers with $b \leqslant 40$ km s^{-1} contribute to the baryon content of the photoionised IGM. For the interval H I column density $10^{13.2} - 10^{16.2}$ cm^{-2}, we find $\Omega(\mathrm{NLy}\alpha) \gtrsim 0.0060$ or $\Omega(\mathrm{NLy}\alpha)/\Omega_{\mathrm{b}} \gtrsim 0.14$, where $\Omega_{\mathrm{b}} = 0.044$, the total baryon density (e.g. Spergel *et al.* 2003). It is a lower limit because absorbers with $\log N(\mathrm{H\ I}) < 13.2$ that are the most numerous are not included. If we assume that the power law fits the data down to the lowest observed column density $\log N(\mathrm{H\ I}) = 12.42$, $\Omega(\mathrm{NLy}\alpha)/\Omega_{\mathrm{b}} \approx 0.28$, i.e. the photoionised IGM contains 28% of the total baryon inventory at $z < 0.5$. This result is consistent with the findings of Penton *et al.* (2004).

To estimate an error on $\Omega(\mathrm{NLy}\alpha)$ remains, however, difficult. It is model dependent, and in particular it assumes that the IGM is isothermal. The representative temperature

https://doi.org/10.1017/S1743921305002565 Published online by Cambridge University Press

itself is not well known, and a large sample of QSO sight-lines would be needed to further constrain the typical IGM temperature. A larger sample coupled with simulations would also better constrain β and Γ_{12}. It is not clear what would be the lowest H I column density to be included in the calculation of Ω(NLyα). Only if the Cosmic Origin Spectrograph (COS) is finally sent into orbit will the S/N be high enough to better statistically detect the weakest Lyα systems and the $f(N_{\rm H\,I})$ distribution down to the lowest H I column densities. Finally, a better understanding of the broad Lyα absorption lines and the fraction of the broadening due solely to thermal motions is required. With the current available spectra, there is no indication of subcomponent structure in the broad Lyα absorption lines. Since we are using several Lyman-series lines for a given absorber, b and N are well constrained. However, if $b_{\rm thermal} \approx 0.7b$ is a good approximation for the amount of thermal broadening and if it holds for absorbers with $b > 40$ km s^{-1}, H I absorbers with b up to 60 km s^{-1} should be considered in the calculation of the $f(N_{\rm H\,I})$ and Ω(NLyα). Doing so, we would find $(\beta, \log C_{\rm H\,I}) = (1.73, 11.4)$ and $\Omega({\rm NLy}\alpha)/\Omega_{\rm b} \approx 0.36$ for $\log N({\rm H\,I}) = [12.42, 16.20]$. If other broadening mechanisms are important, the thermal broadening could drop dramatically for the broad Lyα absorption lines, implying that most of the H I lines would arise in the photoionised IGM, not in the WHIM. If the whole sample is considered, $\Omega({\rm NLy}\alpha)/\Omega_{\rm b}$ could be as high as 42%. Therefore, although the exact baryon content in the photoionised IGM remains uncertain, the photoionised Lyα forest is clearly a large reservoir of baryons that could comprise 30 to 40% of the total baryonic matter. This is indeed much larger than in the galaxies where only ∼9% of the baryons are present (Fukugita *et al.* 1998).

3.2. *Broad Lyα absorption lines*

The remaining baryons certainly reside in the WHIM: shock-heated intergalactic gas with temperatures in the range 10^5 to 10^7 K predicted by cosmological hydrodynamical simulations to contain 30–50% of the baryons at low redshift (Cen & Ostriker 1999; Davé *et al.* 1999). The cosmological mass density of the broad Lyα absorbers in terms of today's critical density can be written (Richter *et al.* 2004, Sembach *et al.* 2004) as,

$$\Omega({\rm BLy}\alpha) \approx 1.667 \times 10^{-23} \frac{\Sigma f_{\rm H}(T_i) N_{\rm H\,I}(i)}{\Sigma \Delta X}, \tag{3.2}$$

where $f_{\rm H}(T)$ is the conversion factor between H I and total H. For our sample, the total absorption distance path is $\Sigma\Delta X = 1.055$. In this expression the sum over index i is a measure of the total hydrogen column density in the broad absorbers. The conversion factor between H I and total H is given by Sutherland & Dopita (1993) for temperatures $10^5 - 10^7$ K assuming collisional ionisation equilibrium:

$$\log f_{\rm H}(T) \approx -13.9 + 5.4 \log T - 0.33 (\log T)^2 . \tag{3.3}$$

We find $\Omega({\rm BLy}\alpha)/\Omega_{\rm b} \approx 0.21$ if $40 < b \leqslant 150$ km s^{-1}. This baryonic density is large and may only be the tip of the iceberg that can be observed with the current data. Indeed with the achieved S/N, only the WHIM regions with the lowest temperature and highest total gas column density can be traced by the broad Lyα absorption lines. The broadest and shallowest Lyα absorption lines where most of baryons would reside are beyond detectability with the STIS sample. Only with COS will we be able to achieve the high S/N high resolution spectra needed to detect the shallowest broad Lyα absorption lines.

Although the baryon estimate via broad H I absorption lines relies on several assumptions, with the most critical one being that the broadening is purely thermal, it does *not* depend on the metallicity. With the current data set, single-component fits provide a reasonable approximation to the observed profiles. Richter *et al.* (in preparation, see also

https://doi.org/10.1017/S1743921305002565 Published online by Cambridge University Press

these proceedings) further discuss the different broadening mechanisms and conclude that thermal broadening is likely to dominate the broadening of the Lyα absorption lines. A larger sample would clearly help and we plan to analyse the remaining QSO sample observed with STIS E140M in order to better characterise the broad and narrow absorption lines.

4. Summary

An analysis of the H I distribution in the low-redshift IGM observed with high quality STIS/E140M and *FUSE* data is presented. Our preliminary conclusions are summarised as follows:

(*a*) STIS/E140M and *FUSE* observations reveal narrow and broad H I absorptions in the low-z IGM that could be tracers of the warm photoionised IGM ($T \lesssim 10^4$ K) and WHIM ($T \sim 10^5 - 10^6$ K), respectively.

(*b*) The Doppler parameter b increases with decreasing redshift.

(*c*) A larger fraction of systems have $b > 40$ km s^{-1} at low-z than at high-z.

(*d*) The observed baryonic content of the low-z IGM is enormous: 30-40% of the baryons are in the cool photoionised IGM, and at least 20% in the warm-hot ionised medium. We note that the shallowest, broadest H I absorptions where most of the baryons could reside are still to be discovered.

We are currently adding several other lines of sight observed with STIS and *FUSE* to improve the statistics in our sample.

References

Bahcall, J. N., Jannuzi, B. T., Schneider, D. P., Hartig, G. F., Bohlin, R., Junkkarinen, V., 1991, ApJ, 377, L5
Cen, R., Ostriker, J. P., 1999, ApJ 514, 1
Davé, R., Hernquist, L., Katz, N., Weinberg, D. H., 1999, ApJ, 511, 521
Davé, R., Tripp, T. M., 2001, ApJ, 553, 528
Fukugita, M., Hogan, C. J., Peebles, P. J. E., 1998, ApJ, 503, 518
Hu, E. M., Kim, T., Cowie, L. L., Songaila, A., Rauch, M., 1995, AJ, 110, 1526
Impey, C. D., Petry, C. E., Flint, K. P., 1999, ApJ, 524, 536
Kim, T.-S., Carswell, R. F., Cristiani, S., D'Odorico, S., Giallongo, E., 2002a, MNRAS, 335, 555
Kim, T.-S., Cristiani, S., D'Odorico, S., 2002b, A&A, 383, 747
Kim, T., Hu, E. M., Cowie, L. L., Songaila, A., 1997, AJ, 114, 1
Lu, L., Sargent, W. L. W., Womble, D. S., Takada-Hidai, M., 1996, ApJ, 472, 509
Nicastro, F., *et al.*, 2005, Nature, 433, 495
Penton, S. V., Shull, J. M., Stocke, J. T., 2000, ApJ, 544, 150
Penton, S. V., Stocke, J. T., Shull, J. M., 2004, ApJS, 152, 29
Richter, P., Savage, B. D., Tripp, T. M., Sembach, K. R., 2004, ApJS, 153, 165
Savage, B. D., Lehner, N., Wakker, B. P., Sembach, K. R., Tripp, T. M., 2005, ApJ, in press [astro-ph/0503051]
Schaye, J., 2001, ApJ, 559, 507
Sembach, K. R., Tripp, T. M., Savage, B. D., Richter, P., 2004, ApJS, 155, 351
Shull, J.-M., *et al.*, 2000, ApJ, 538, L13
Spergel, D. N., *et al.*, 2003, ApJS, 148, 175
Sutherland, R. S., Dopita, M. A., 1993, ApJS, 88, 253
Tripp, T. M., Bowen, D. V., Sembach, K. R., Jenkins, E. B., Savage, B. D., Richter, P., 2004, [astro-ph/0411151]
Weymann, R. J., *et al.*, 1998, ApJ, 506, 1